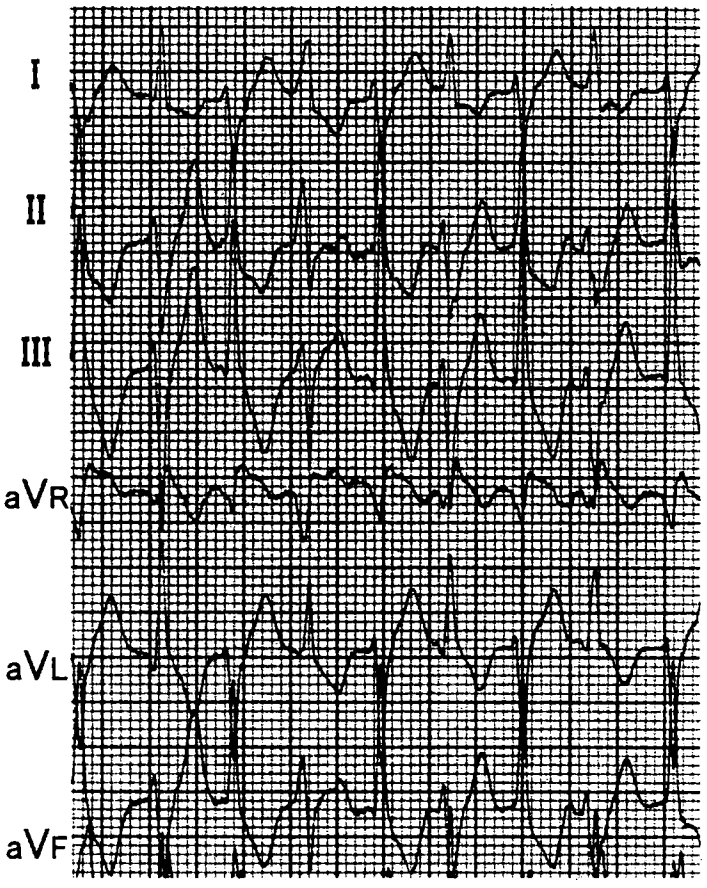

図2　トレッドミル運動負荷時の四肢誘導記録

臨床経過

電気生理検査(EPS)では，プログラム刺激で基本刺激間隔600 msecと400 msecで2連発早期刺激(刺激間隔200 msまで)を行い，イソプロテレノール40 μg/hr，エピネフリン200 μg/hr負荷下にても心室頻拍は誘発されなかった．カルベジロール(5 mg)内服時のトレッドミル試験(Bruce protocol)では3 METs，HR100 bpmにてVPCの散発，7 METsにて心拍数100/分程度(coupling interval 320 msec)の双方向性心室頻拍が誘発されたため負荷を中止した(図2)．血圧は安静時106/72 mmHg，双方向性心室頻拍時にて117/76 mmHgであった．意識消失，胸部症状，呼吸困難感等の自覚症状はなかった．エピネフリンの経静脈負荷試験を行ったところ，0.2 μg/kg/minで心拍数74/分程度の洞調律から多形性心室頻拍が誘発された(図3)が，血圧変化は安静時と比較し明らかでなかった．ノルエピネフリン負荷ではPVCの散発が観察され，血圧165/95 mmHgとなり胸部不快感が出現した．以上よりCPVTと診断し，ICD移植術を施行した．設定はβ遮断薬内服で徐脈を呈していたためDDI 60 bpmとし，VT rate 140 bpmに対してはモニタリングのみ行い，VF rate 190 bpmに対して31 J通電を7回行う設定とした．頻拍停止後，back up pacing 60 bpmとした．その後，メトプロロール60 mg/日でトレッドミル試験をしたところ，やはり多源性VPCが出現したため90 mgに増量し退院した．2ヵ月後のトレッドミル試験にて心拍数80/分程度からVPC散発したためさらに内服を120 mg/日へ増量し経過をみていたが，3ヵ月後，運動時の心室頻拍に対しICDが作動し，31 Jの通電1回で洞調律に復帰した．

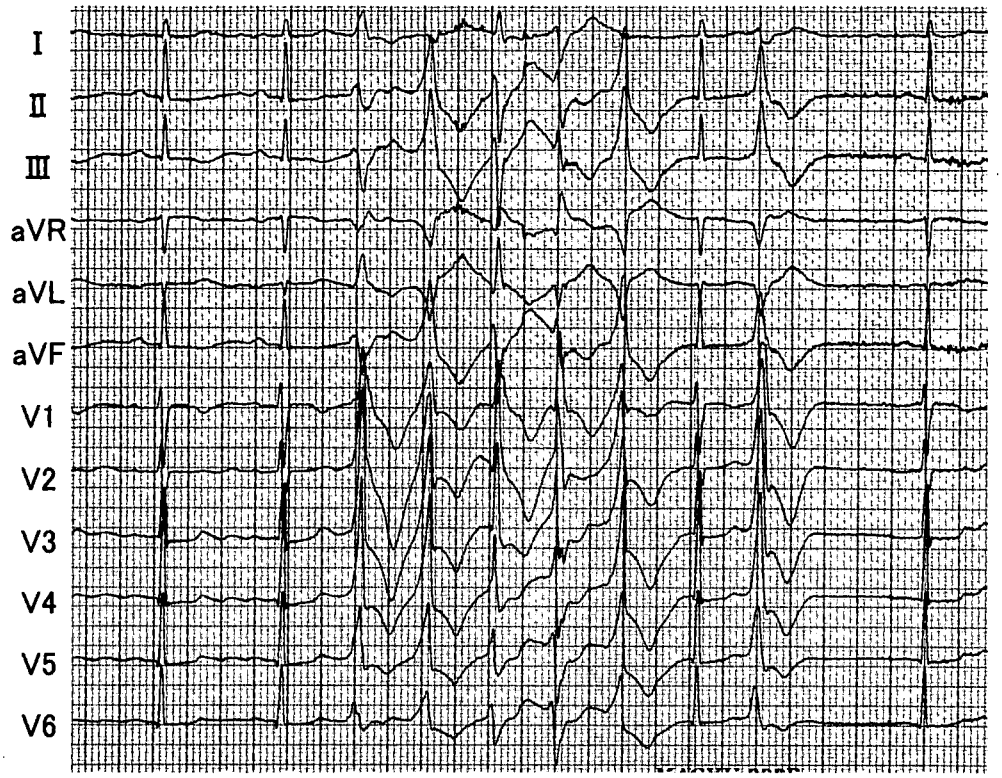

図3　エピネフリン負荷時に観察された多形性心室頻拍

遺伝子検査

リアノジン受容体は約5000アミノ酸からなる巨大分子が4量体となって形成されており，その遺伝子（RyR_2）は105個のエクソンからなる．われわれはCPVTを発症する頻度の高い29個のエクソン（central domain：44～49，C-terminal domain：83～105）について，PCR法にて増幅しDHPLC法によりRyR_2変異のスクリーニングを行った．DHPLC法にてエクソン94に異常な2峰性の波形を認め（図4A），DNAシークエンスでは13759番目のアデニン（A）がグアニン（G）に変わるミスセンス変異を認め，4587番目のアミノ酸はイソロイシン（I）からバリン（V）に変わっていた（図4B）．また，この患者の10才の長女と8才の長男にはRyR_2検査の同意が得られず行えていないが，トレッドミル試験では心室頻拍の出現は認めなかった．

Ⅲ．考　　察

典型的な臨床経過を示したCPVT成人例で，RyR_2の変異を発見した．4587番目のアミノ酸がイソロイシン（I）からバリン（V）に置換するミスセンス変異（I4587 V）で，いままでに報告のないものであった．CPVTは運動負荷・心的ストレスによって多形性心室頻拍が誘発される予後不良の疾患で，典型例は小児期に失神発作で発見され，突然死の原因となると考えられ[1)~4)]，最初の発作が致死的となる場合があり，女性より男性で予後不良とされている．また安静時心電図に異常所見がないため，てんかんや副交感神経反射などと誤診されている例も多い．

CPVT患者では心筋のCa制御異常を起こすと考えられる心筋リアノジン受容体とcarsequestrinの遺伝子変異が報告されている．このうち心筋リアノジン受容体は筋小胞体膜に発現しCa induced-Ca releaseを制御しているチャネルである．運動や精神

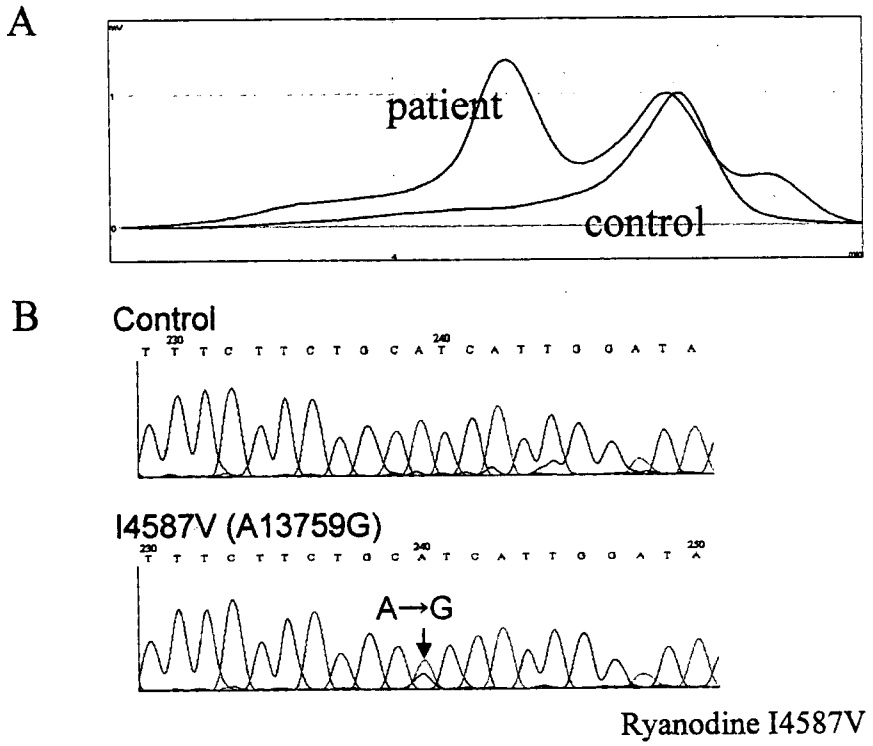

図4　遺伝子検索結果

A：DHPLC法によるRYR2の異常検出.

B：異常パターンを示したCDNAフラグメントの塩基配列．上に正常例からの結果を示す.

的ストレスでβ受容体を介した細胞内cAMPが増加すると，phosphokinaseA(A-kinase)によるL型カルシウムチャネルのリン酸化の結果，細胞内へのCaイオンの流入が増加する．これに呼応して，筋小胞体リアノジン受容体チャネルを介したカルシウム放出が促進される．カルシウム放出にはFK-BPのA-kinseによるリアノジン受容体蛋白のリン酸化が関与している．本例で発見された*RyR*$_2$変異は，リアノジン受容体の膜貫通領域でCaイオンを通すpore部分に位置しており，リアノジン受容体は機能障害をきたしていると推測される.

リアノジン受容体チャネルによる筋小胞体からのカルシウム放出の制御に支障が生じて，細胞内カルシウム過負荷が起こり遅延後脱分極(DAD)が増強しtriggered activityから致死性心室性不整脈(CPVT)が出現する可能性がある．CPVTの治療としてはβ遮断薬が有効であるが，治療抵抗性の症例も多く存在し，β遮断薬による治療中であっても突然死した報告もある[2]．Cerroneらは，リアノジン受容体の膜貫通領域に遺伝子変異(*R4496C*)を導入した遺伝子改変マウスにおいてβ遮断薬は心室性頻拍を抑制しなかった[11]としており，このことからもリアノジン受容体の異常によるCPVTの治療としてβ遮断薬だけでは不十分であると考えられる．実際，本例のCPVTは，上述のようにβ遮断薬に抵抗性であった．また常染色体優性の遺伝形式をとる遺伝性CPVT患者においてはカルシウム遮断薬が心室頻拍を抑制したとの報告もある[2]が，突然死を防ぐことは出来なかった.

これまでの報告によると，FK-BP12.6結合部位を含むcentral domainと[13]膜貫通領域を含むC-terminal domainに遺伝子変異を持つCPVTがほとんどである[14]．しかし，本症例ではリアノジン受容体の膜貫通領域に遺伝子異常が存在した．先天性

QT延長症候群の1型と2型では，pore site含む膜貫通領域に遺伝子変異を持つと重症であるとの報告があり[15),16)]，CPVT患者においても同様にリアノジン遺伝子のうち膜貫通領域に遺伝子変異があると，β遮断薬などの薬剤に治療抵抗性を有するため多形性VTから突然死をきたしやすくなるのかもしれない．今後，CPVTの重症度の指標や治療法の選択において遺伝子検索が重要な意味を持つ可能性が考えられ，さらに多くの症例で検討する必要があると思われる．

CPVT症例の突然死を防ぐ最も確実な方法はICD植込みである．本症例もβ遮断薬抵抗性の運動誘発性心室性不整脈であったためICD移植を行った．ICD移植後，運動時の心室頻拍に対して作動が認められた．CPVTに対するICD植込み後の長期予後についてはいまだ不明であり，今後の検討が必要と考えられる．

〔文　献〕

1) Leenhardt A, Lucet V, Denjoy I Grau F, Ngoc DD, Coumel P : Catecholaminergic polymorphic ventricular tachycardia in children. A7-year follow-up of 21 patients. Circulation, 1995 ; 91 : 1512～1519
2) Coumel P : Polymorphous ventricular tachyarrhythmias in the absence of structural heart disease. Pacing Clin Electrophysiol, 1997 ; 20 : 2065～2067
3) Priori SG, Napolitano C, Memmi M, Colombi B, Drago F, Gasparini M, DeSimone L, Coltorti F, Bloise R, Keegan R, Cruz Filho FE, Vignati G, Benatar A, DeLogu A : Clinical and molecular characterization of patients with catecholaminergic polymorphic ventricular tachycardia. Circulation, 2002 ; 106 : 69～74
4) Sumitomo N, Harada K, Nagashima M, Yasuda T, Nakamura Y, Aragaki Y, Saito A, Kurosaki K, Jouo K, Koujiro M, Konishi S, Matsuoka S, Oono T, Hayakawa S, Miura M, Ushinohama H, Shibata T, Niimura I : Catecholaminergic polymorphic ventricular tachycardia : Electrocardiographic characteristics and optimal therapeutic strategies to prevent sudden death. Heart, 2003 ; 89 : 66～70
5) Tester DJ, Spoon DB, Valdivia HH, Makielski JC, Ackerman MJ : Targeted mutational analysis of the RyR2-encoded cardiac ryanodine receptor in sudden unexplained death : a molecular autopsy of 49 medical examiner/coroner's cases. Mayo Clin Proc, 2004 ; 79 : 1380～1384
6) Laitinen PJ, Brown KM, Piippo K, Swan H, Devaney JM, Brahmbhatt B, Donarum EA, Marino M, Tiso N, Vitasalo M, Toivonen L, Stephan DA, Kontula K : Mutations of the cardiac ryanodine receptor (RyR2) gene in familial polymorphic ventricular tachycardia. Circulation, 2001 ; 103 : 485～490
7) Priori SG, Napolitano C, Tiso N, Memmi M, Vignati G, Bloise R, Sorrentino V, Danieli GA : Mutations in the cardiac ryanodine receptor gene (hRyR2) underlie catecholaminergic polymorphic ventricular tachycardia. Circulation, 2001 ; 103 : 196～200
8) Laitinen PJ, Swan H, Kontula K : Molecular genetics of exercise-induced polymorphic ventricular tachycardia : identification of three novel cardiac ryanodine receptor mutations and two common calsequestrin 2 amino-acid polymorphisms. Eur J Hum Genet, 2003 ; 11 : 888～891
9) Postma AV, Denjoy I, Hoorntje TM, Lupoglazoff JM, Da Costa A, Sebillon P, Mannens MM, Wilde AA, Guicheney P : Absence of calsequestrin 2 causes severe forms of catecholaminergic polymorphic ventricular tachycardia. Circ Res, 2002 ; 91 : e21～e26
10) Viatchenko-Karpinski S, Terentyev D, Gyorke I, Terentyeva R, Volpe P, Priori SG, Napolitano C, Nori A, Williams SC, Gyorke S : Abnormal calcium signaling and sudden cardiac death associated with mutation of calsequestrin. Circ Res, 2004 ; 94 : 471～477
11) Cerrone M, Colombi B, Santoro M, di Barletta MR, Scelsi M, Villani L, Napolitano C, Priori SG : Bidirectional ventricular tachycardia and fibrillation elicited in a knock-in mouse model carrier of a mutation in the cardiac ryanodine receptor. Circ Res, 2005 ; 96 : e77～e82
12) Wehrens XH, Lehnart SE, Marks AR : Ryanodine receptor-targeted anti-arrhythmic therapy. Ann N Y Acad Sci, 2005 ; 1047 : 366～375
13) Aizawa Y, Ueda K, Komura S, Washizuka T, Chinushi M, Inagaki N, Matsumoto Y, Hayashi T, Takahashi M, Nakano N, Yasunami M, Kimura A, Hiraoka M, Aizawa Y : A novel mutation in FKBP12.6 binding region of the human cardiac ryanodine receptor gene (R2401H) in a Japanese patient with catecholaminergic polymorphic ventricular tachycardia. Int J Cardiol, 2005 ; 99 : 343～345
14) Bagattin A, Veronese C, Bauce B, Wuyts W, Settimo L, Nava A, Rampazzo A, Danieli GA : Denaturing HPLC-based approach for detecting RYR2 mutations involved in malignant arrhythmias. Clin Chem, 2004 ; 50 : 1148～

1155
15) Shimizu W, Horie M, Ohno S, Takenaka K, Yamaguchi M, Shimizu M, Washizuka T, Aizawa Y, Nakamura K, Ohe T, Aiba T, Miyamoto Y, Yoshimasa Y, Towbin JA, Priori SG, Kamakura S : Mutation site-specific differences in arrhythmicrisk and sensitivity to sympathetic stimulation in the LQT1 form of congenital long QT syndrome multicenter study in Japan. J Am Coll Cardiol. 2004 ; 44 : 117～125
16) Moss AJ, Zareba W, Kaufman ES, Gartman E, Peterson DR, Benhorin J, Towbin JA, Keating MT, Priori SG, Schwartz PJ, Vincent GM, Robinson JL, Andrews ML, Feng C, Hall WJ, Medina A, Zhang L, Wang Z : Increased risk of arrhythmic events in long-QT syndrome with mutations in the pore region of the human ether-a-go-go-related gene potassium channel. Circulation. 2002 ; 105 : 794～799

III 不整脈

Jervell and Lange-Nielsen症候群

Jervell and Lange-Nielsen syndrome

Key words：Jervell and Lange-Nielsen症候群，KCNQ1，KCNE1，QT延長症候群，torsade de pointes

堀江 稔

1. 概念・定義

Jervell and Lange Nielsen症候群(JLNS)は，主として常染色体劣性遺伝で，QT延長と先天性の両側聾を伴う非常にまれな疾患である[1]．いわゆる常染色体優性遺伝を示すQT延長症候群であるRomano Ward症候群(RWS)よりも，一般に心臓症状は重篤であり，幼少時から失神や突然死を起こすことが知られている．1957年，JervellとLange-Nielsen[2]は，ノルウェー人の家系で，血族結婚ではない両親から生まれた6人の子供のうち4人が心電図上，著しいQT延長と両側聾を呈し，幼少時から繰り返す失神を起こして，更に，うち3人が各々4，5，9歳時に突然死したと報告した．これが，本症候群の最初の臨床報告とされており，その後，多くのレポートがこれに続き，血族結婚で多く常染色体劣性遺伝を主とする病態であることが示された[3]．しかしながら，初期の症例報告[1]では，患者家族にも軽度のQT延長が認められる者もある．昨年，Schwartz，著者ら[39]はJLNSの187人をまとめて，その詳細を報告したが，86％が有症状であり，その半数は3歳時既に発症していた．平均QTc時間は著しく延長しており，心イベントの95％は，LQT1と同じく運動や感情的興奮に伴って発症していた．βブロッカーはRWSの場合より，無効なことが多く，27％に突然死が認められた．

2. 病因と病態

一方，1995年以降の精力的なQT延長症候群の原因遺伝子の検索の結果，JLNSの責任遺伝子も，ある種のRWSと同様，心筋の再分極過程をつかさどるカリウム・チャネルをコードする遺伝子の変異によるカリウム・チャネルのloss-of-function型の機能障害が惹起されて，その結果，発症することが明らかとなった．すなわち，心筋活動電位の再分極が著しく遅れるために，特異的な多形性心室頻拍(torsade de pointes: TdP)が誘発され，まれならず心室細動となり，突然死を来すことがわかってきた[5,6]．心室筋の再分極過程には，主に2種類のカリウム・チャネルが関与しているが，そのうち遅い活性化を示す遅延整流カリウム・チャネルは，2つの遺伝子すなわちKCNQ1とKCNE1によりコードされI_{Ks}電流を運ぶ[7,8]．同じカリウム・チャネルは，内耳に発現しており，内リンパ液のカリウム濃度維持に，必須の働きをしている．このチャネルが完璧に障害されるため，先天性の両側聾が発症する．

1997年以降，JLNSの症例で，KCNQ1あるいはKCNE1遺伝子のホモあるいはヘテロ変異が次々と発見された[9-12]．**表1**に現在，報告されているJLNS関連の変異をまとめる．Neyroudらの最初の報告は，2家系のJLNSで3人の子供にKCNQ1のC末端の変異を発見したというものである．まだ，議論の余地はあるが，RWSでは，一般にC末端の変異の臨床像は軽微であるとされ，実際，この2家系のヘテロ接合症例はすべて無症候性であった[13-15]．

一方，Splawskiら[10]が報告した大きなJLNS家系では，KCNQ1のS2-S3リンカー部分のホ

Minoru Horie: Department of Cardiovascular and Respiratory Medicine, Shiga University of Medical Science 滋賀医科大学 呼吸循環器内科

0047-1852/07/¥40/頁/JCLS

表1　JLNSの遺伝子異常

塩基配列	アミノ酸変化	部位	変異のタイプ	ヘテロキャリアの症状	そのQTc時間	参考文献
KCNQ1						
451-452delCT	A150fs+132	S2	FS/del	none	N	16
477+1 G>A	M159sp	S2	SE	unknown	unknown	17
477+5 G>A	M159sp	S2	SE	none	N, B, P	18
C513G	Y171X	S2-S3	NS	none	N, B	19, 20
567insG	G189fs+94	S2-S3	FS/ins	syncope, SD	B, P	10
572-576del	L191fs+90	S2-S3	FS/del	syncope	N, B, P	21-23
585delG	R195fs+40	S2-S3	FS/del	none	N	20
G604A	D202N	S3	MS	none	B, P	20
G728A	R243H	S4-S5	MS	unknown	N, B	18, 22
G783C	E261D	S4-S5	MS	none	N	23, 24
G806A	G269D	S5	MS	none	N, B, P	20
G914C	W305S	pore	MS	none	N, B	25
1008delC	A336fs+16	S6	FS/del	none	N	24
1188delC	I396fs+21	C-term	FS/del	unknown	unknown	26
C1552T	R518X	C-term	NS	normal	N, B	23, 26, 27
C1588T	Q530X	C-term	NS	none	N	2, 23, 24
1630 del6/ins7	E543fs+107	C-term	FS/del/ins	none	N, B, P	9
C1760T	T587M	C-term	MS	*de novo*	(−)	28
G1766A	G589D	C-term	MS	none	N, B, P	19
G1781A	R594Q	C-term	MS	none	N	24
1892del20	P630fs+13	C-term	FS/del	none	N	28
KCNE1						
C20T/G226A	T7I/G38S	N-term/pore	double MS	none	N	11
G254A	N76D	C-term	MS	syncope	P	12
—	T59P/L60P	transmembrane	double MS	unknown	unknown	24

del: 欠損, ins: 挿入, FS: フレームシフト, SE: スプライシング異常, NS: stop codonとなるノンセンス変異, MS: ミスセンス変異, SD: 突然死

N, B, Pの定義；N: normal QTc<450 ms, B: borderline QTc 450-480 ms, P: prolonged QTc>480 ms

モ変異(567insG)が発端者に発見されているが，その家族にも突然死を含む症候性のQT延長が認められた．このように遺伝子変異に依存して，そのJLNS家族内の臨床像は，非常に異なり，心電図で判定されるQT時間もばらつくようであるが，報告をみるかぎり，症候性のヘテロ変異キャリアは，もう1つだけであり，それもKCNQ1のS2-S3リンカーの572-576del変異であった．発端者の家族で検索された13人のうち，1人だけが発症していた．著者らも，感音性聴音障害を有し，6歳時から繰り返すTdPによる失神を起こす女性例でKCNQ1のS4-S5リンカー変異を発見したが，調べ得たかぎりでは，失神や突然死などの家族歴はなく，QT時間も正常範囲内であった．

更に，頻度は少ないがKCNE1ホモ変異によるJLNS症例のヘテロ変異キャリアは，無症候性であり，したがって，JLNSの発端者は，RWSのそれよりも一般的には，臨床像が重篤であり，その家族の変異キャリアは，無症候性であることがいえる．その説明として，ヘテロでも発症するような重症タイプの変異がホモ接合の場合，embryonic deathとなる可能性がある．

3. 診断と鑑別診断

前述のような兆候から，JLNSの診断は容易

であり，先天性の両側聾からRWSとの鑑別は簡単である．遺伝子検索では，その責任遺伝子がKCNQ1かKCNE1であるとわかっているため診断率は高く，次に述べる治療との関連からも，遺伝子検査は家族を含めて行うべきである．

4. 治療と予後

一般的に，JLNSは幼少時よりTdP発作を起こし，RWSよりも生命予後は不良とされる[29]．薬物療法としてはβブロッカーが有用であるが，一度でもTdPあるいは失神発作があるようであれば，原則，ICD治療(あるいはhome AED)を考慮する．病因と病態のところでも論じたように，家族のヘテロ変異キャリアの場合，QT延長を来す薬剤や低カリウム血症などの誘因があると，いわゆるカリウム電流の予備能(K current reserve)が少ないために，QT時間が正常ボーダーラインのような場合でも，TdPを発症するリスクが健常者に比べて高い．したがって，予期せぬ心臓突然死を予防するためにも，遺伝子検査が重要である．

文　献

1) Schwartz PJ, et al: The long Q-T syndrome. Am Heart J **89**: 378-390, 1975.
2) Jervell A, Lange-Nielsen F: Congenital deaf-mutism, functional heart disease with prolongation of the Q-T interval and sudden death. Am Heart J **54**: 59-68, 1957.
3) Fraser GR, et al: Congenital deafness associated with electrocardiographic abnormalities, fainting attacks and sudden death. A recessive syndrome. Q J Med **33**: 361-385, 1964.
4) Jervell A, et al: The surdo-cardiac syndrome: three new cases of congenital deafness with syncopal attacks and Q-T prolongation in the electrocardiogram. Am Heart J **72**: 582-593, 1966.
5) Dessertenne F: Un chapitre nouveau d'electrocardiographie: Les variations progressive de l'amplitude de l'electrocardiogramme. Actual Cardiol Angeiol Int **15**: 241-249, 1966.
6) Roden DM, et al: Multiple mechanisms in the long-QT syndrome. Current knowledge, gaps, and future directions. The SADS Foundation Task Force on LQTS. Circulation **94**: 1996-2012, 1996.
7) Barhanin J, et al: KvLQT1 and lsK(minK) proteins associate to form the I_{Ks} cardiac potassium current. Nature **384**: 78-80, 1996.
8) Sanguinetti MC, et al: Coassembly of KvLQT1 and minK(IsK) proteins to form cardiac I_{Ks} potassium channel. Nature **384**: 80-83, 1996.
9) Neyroud N, et al: A novel mutation in the potassium channel gene *KVLQT1* causes the Jervell and Lange-Nielsen cardioauditory syndrome. Nat Genet **15**: 186-189, 1997.
10) Splawski I, et al: Molecular basis of the long-QT syndrome associated with deafness. N Engl J Med **336**: 1562-1567, 1997.
11) Schulze-Bahr E, et al: *KCNE1* mutations cause Jervell and Lange-Nielsen syndrome. Nat Genet **17**: 267-268, 1997.
12) Duggal P, et al: Mutation of the gene for IsK associated with both Jervell and Lange-Nielsen and Romano-Ward forms of long-QT syndrome. Circulation **97**: 142-146, 1998.
13) Donger C, et al: KVLQT1 C-terminal missense mutation causes a forme fruste long-QT syndrome. Circulation **96**: 2778-2781, 1997.
14) Moss AJ, et al: Increased risk of arrhythmic events in long-QT syndrome with mutations in the pore region of the human ether-a-go-go-related gene potassium channel. Circulation **105**: 794-799, 2002.
15) Shimizu W, et al: Mutation site-specific differences in arrhythmic risk and sensitivity to sympathetic stimulation in the LQT1 form of congenital long QT syndrome. J Am Coll Cardiol **44**: 117-125, 2004.
16) Chen Q, et al: Homozygous deletion in *KVLQT1* associated with Jervell and Lange-Nielsen syndrome. Circulation **99**: 1344-1347, 1999.
17) Splawski I, et al: Spectrum of mutations in long-QT syndrome genes. *KVLQT1*, *HERG*, *SCN5A*, *KCNE1*, and *KCNE2*. Circulation **102**: 1178-1185, 2000.

18) Chouabe C, et al: Novel mutations in KvLQT1 that affect I_{Ks} activation through interactions with Isk. Cardiovasc Res **45**: 971-980, 2000.
19) Piippo K, et al: A founder mutation of the potassium channel KCNQ1 in long QT syndrome: implications for estimation of disease prevalence and molecular diagnostics. J Am Coll Cardiol **37**: 562-568, 2001.
20) Wang Z, et al: Compound heterozygous mutations in *KvLQT1* cause Jervell and Lange-Nielsen syndrome. Mol Genet Metab **75**: 308-316, 2002.
21) Huang L, et al: A spectrum of functional effects for disease causing mutations in the Jervell and Lange-Nielsen syndrome. Cardiovasc Res **51**: 670-680, 2001.
22) Tyson J, et al: IsK and KvLQT1: mutation in either of the two subunits of the slow component of the delayed rectifier potassium channel can cause Jervell and Lange-Nielsen syndrome. Hum Mol Genet **6**: 2179-2185, 1997.
23) Tranebjaerg L, et al: Jervell and Lange-Nielsen syndrome: a Norwegian perspective. Am J Med Genet **89**: 137-146, 1999.
24) Tyson J, et al: Mutational spectrum in the cardioauditory syndrome of Jervell and Lange-Nielsen. Hum Genet **107**: 499-503, 2000.
25) Neyroud N, et al: Heterozygous mutation in the pore of potassium channel gene *KvLQT1* causes an apparently normal phenotype in long QT syndrome. Eur J Hum Genet **6**: 129-133, 1998.
26) Wei J, et al: Novel *KCNQ1* mutations associated with recessive and dominant congenital long QT syndromes: evidence for variable hearing phenotype associated with R518X. Hum Mutat **15**: 387-388, 2000.
27) Ning L, et al: Novel compound heterozygous mutations in the KCNQ1 gene associated with autosomal recessive long QT syndrome (Jervell and Lange-Nielsen syndrome). Ann Noninvasive Electrocardiol **8**: 246-250, 2003.
28) Neyroud N, et al: Genomic organization of the *KCNQ1* K^+ channel gene and identification of C-terminal mutations in the long-QT syndrome. Circ Res **84**: 290-297, 1999.
29) Schwartz PJ, et al: The Jervell and Lange-Nielsen syndrome: natural history, molecular basis, and clinical outcome. Circulation **113**: 783-790, 2006.

Dominant Negative Suppression of Rad Leads to QT Prolongation and Causes Ventricular Arrhythmias via Modulation of L-type Ca^{2+} Channels in the Heart

Hirotaka Yada, Mitsushige Murata, Kouji Shimoda, Shinsuke Yuasa, Haruko Kawaguchi, Masaki Ieda, Takeshi Adachi, Mitsuru Murata, Satoshi Ogawa, Keiichi Fukuda

Abstract—Disorders of L-type Ca^{2+} channels can cause severe cardiac arrhythmias. A subclass of small GTP-binding proteins, the RGK family, regulates L-type Ca^{2+} current ($I_{Ca,L}$) in heterologous expression systems. Among these proteins, Rad (Ras associated with diabetes) is highly expressed in the heart, although its role in the heart remains unknown. Here we show that overexpression of dominant negative mutant Rad (S105N) led to an increase in $I_{Ca,L}$ and action potential prolongation via upregulation of L-type Ca^{2+} channel expression in the plasma membrane of guinea pig ventricular cardiomyocytes. To verify the in vivo physiological role of Rad in the heart, a mouse model of cardiac-specific Rad suppression was created by overexpressing S105N Rad, using the α-myosin heavy chain promoter. Microelectrode studies revealed that action potential duration was significantly prolonged with visible identification of a small plateau phase in S105N Rad transgenic mice, when compared with wild-type littermate mice. Telemetric electrocardiograms on unrestrained mice revealed that S105N Rad transgenic mice had significant QT prolongation and diverse arrhythmias such as sinus node dysfunction, atrioventricular block, and ventricular extrasystoles, whereas no arrhythmias were observed in wild-type mice. Furthermore, administration of epinephrine induced frequent ventricular extrasystoles and ventricular tachycardia in S105N Rad transgenic mice. This study provides novel evidence that the suppression of Rad activity in the heart can induce ventricular tachycardia, suggesting that the Rad-associated signaling pathway may play a role in arrhythmogenesis in diverse cardiac diseases. (***Circ Res.*** **2007;101:69-77.)**

Key Words: G protein ■ L-type Ca^{2+} channels ■ arrhythmia

Rad (Ras associated with diabetes) is the prototypic member of the newly emerging RGK family of proteins, a group of Ras-related GTPases that includes Rad, Gem, and Rem.[1] Rad was initially identified by subtraction cloning as an mRNA overexpressed in skeletal muscle in a subset of patients with type 2 diabetes mellitus.[2] Among the RGK proteins, Rad is abundantly expressed in skeletal and cardiac muscle.[2] It interacts with various signal transduction molecules such as Rho kinase, calmodulin, and calmodulin-dependent protein kinase II, leading to inhibition of their downstream signals.[3–5] In epithelial or fibroblastic cells, overexpression of Rad results in stress fiber and focal adhesion disassembly, implicating an involvement in cytoskeletal regulation through the Rho kinase pathway.[3] In vascular smooth muscle cells, focal gene transduction of Rad attenuates neointimal formation after balloon injury by inhibiting smooth muscle proliferation and migration activated through the Rho kinase pathway.[6] Furthermore, overexpression of Rad in skeletal muscle worsens diet-induced insulin resistance and glucose intolerance, which is consistent with the observed upregulation of Rad in diabetic patients.[7] Despite the critical roles of Rad in diverse biological processes, its function in the heart is still unknown.

Recently, RGK proteins were found to suppress voltage-gated L-type Ca^{2+} currents ($I_{Ca,L}$) in heterologous expression systems and insulin-secreting β cells of the pancreas.[8–10] This was shown to occur via an interaction with Ca^{2+} channel β subunits, and the finding suggests that Rad may play an important role in cellular Ca^{2+} homeostasis. Indeed, overexpression of Gem in PC12 cells and MIN6 cells prevents Ca^{2+}-triggered exocytosis via inhibition of L-type Ca^{2+} channels.[11] In the heart, Ca^{2+} is essential for electrical activity and is a direct activator of the myofilaments in contraction. Among the many Ca^{2+} handling proteins, cardiac L-type Ca^{2+} channels play central roles in initiation of excitation–contraction coupling and in cardiac electrophysiological properties. Abnormal function of Rad in the heart might therefore lead to various cardiac disorders such as arrhythmias or contractile dysfunction.

Original received December 9, 2006; revision received April 10, 2007; accepted May 15, 2007.

From the Cardiopulmonary Division (H.Y., S.Y., M.I., S.O.), Department of Laboratory Medicine (Mitsushige M., Mitsuru M.), Animal Laboratory Center (K.S.), Department of Regenerative Medicine and Advanced Cardiac Therapeutics (H.K., K.F.), and Department of Biochemistry and Integrative Medical Biology (T.A.), School of Medicine, Keio University, Tokyo, Japan.

Correspondence to Mitsushige Murata, MD, PhD, Department of Laboratory Medicine, Keio University, 35 Shinanomachi, Shinjuku-ku, Tokyo 160-8582, Japan. E-mail muratam@cpnet.med.keio.ac.jp

Circulation Research is available at http://circres.ahajournals.org DOI: 10.1161/CIRCRESAHA.106.146399

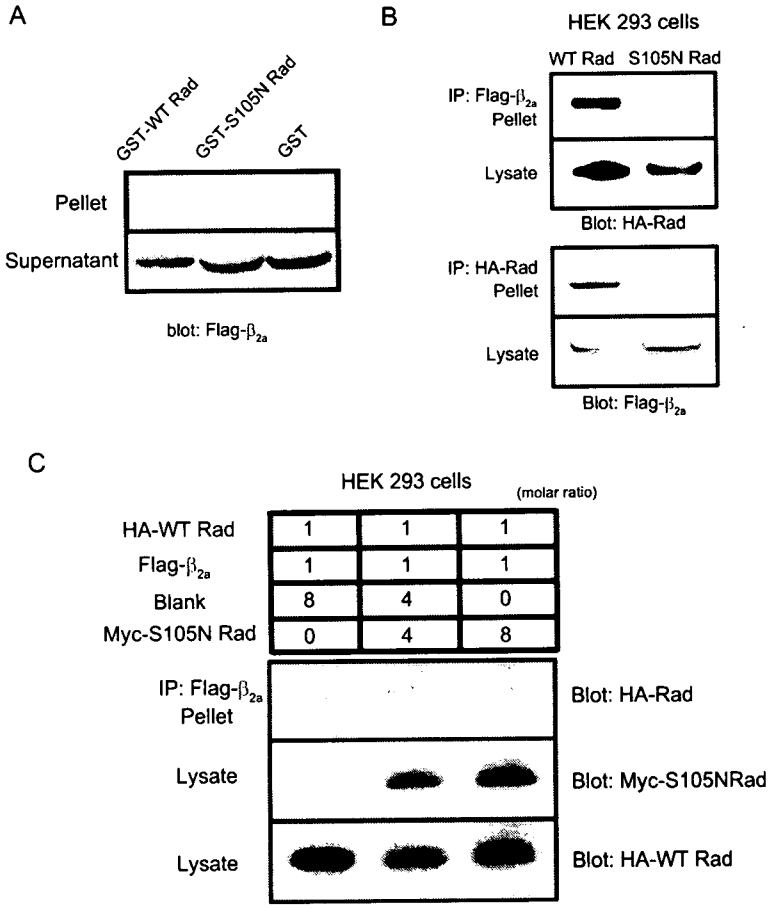

Figure 1. Interaction between Rad and the L-type Ca^{2+} channel β subunit. A, In vitro binding between β_{2a} subunit and WT Rad or S105N Rad. Lysates from Cos7 cells transiently transfected with purified recombinant GST-WT Rad or GST-S105N Rad were incubated with glutathione–Sepharose beads. B, In vivo binding between β_{2a} subunit and WT Rad or S105N Rad. HEK293 cells were cotransfected with hemagglutinin (HA)-tagged Rad and Flag-tagged β_{2a} subunits. The cell lysate was subjected to immunoprecipitation and visualized by immunoblotting with antibodies as indicated. C, Dose-dependent inhibition of the interaction between WT Rad and β subunit by overexpression of S105N Rad. The table denotes the molar ratio of transfected plasmid.

We show here that dominant negative suppression of Rad led to the enhancement of $I_{Ca,L}$ by facilitating channel expression in the plasma membrane of cardiomyocytes, resulting in prolongation of the action potential. Furthermore, transgenic mice with heart-specific overexpression of dominant negative mutant Rad (S105N) displayed ventricular arrhythmias as a consequence of QT prolongation. Our results constitute the first evidence that Rad plays an important role in regulating cardiac electrophysiological properties and that Rad could be a key molecule for understanding the mechanism of arrhythmogenesis in cardiovascular diseases.

Materials and Methods

All experimental procedures and protocols were approved by the Animal Care and Use Committee of Keio University and conformed to the NIH *Guide for the Care and Use of Laboratory Animals*. An expanded Materials and Methods section is available in the online data supplement at http://circres.ahajournals.org.

Myocyte Isolation and Cultures

Myocytes were isolated from the left ventricles of adult guinea pigs and mice using enzymatic digestions as previously described, with slight modifications.[12,13] After isolation, ventricular myocytes were cultured in DMEM containing 10% FBS and 1% penicillin–streptomycin (all from Invitrogen, Carlsbad, Calif) for 24 hours.

Production of S105N Rad Transgenic Mouse

The complete mutant mouse S105N Rad (with the serine at the 105-aa position substituted to arginine, to inhibit GTP binding) cDNA construct was subcloned into the region downstream of the α-myosin heavy chain promoter[14] previously subcloned into the PBS2 SK+ plasmid. The complete transgene was isolated using *Not*I digestion of the PBS2 SK+ plasmid. Transgenic mice were generated by the Animal Laboratory Center of Keio University by cDNA microinjection of fertilized C57BL/6×SJL oocytes using standard techniques.

Statistical Analysis

All data are shown as means±SEM. Statistical differences were determined using repeated-measures ANOVA, and $P<0.05$ was considered significant.

Results

Rad Interacts With L-Type Ca^{2+} Channel β Subunits

Previous reports have shown that Rad interacts with Ca^{2+} channel β subunits in heterologous expression systems, resulting in the inhibition of $I_{Ca,L}$.[15,16] To examine whether Rad physically interacts with the β subunits, glutathione *S*-transferase (GST) pull-down assays were performed. As shown in Figure 1A, recombinant GST wild-type (WT) Rad bound to the β subunits in whole-cell extracts derived from transfected Cos7 cells, whereas GST-S105N Rad did not. Furthermore, interaction between Rad and β subunits was confirmed in the context of the cellular environment. HEK293 cells were transiently transfected with Flag-tagged β_{2a} subunits and hemagglutinin-tagged WT Rad or S105N Rad. After 24 hours in culture, coimmunoprecipitation assays were performed. Consistent with the previous report,[15] the β_{2a}

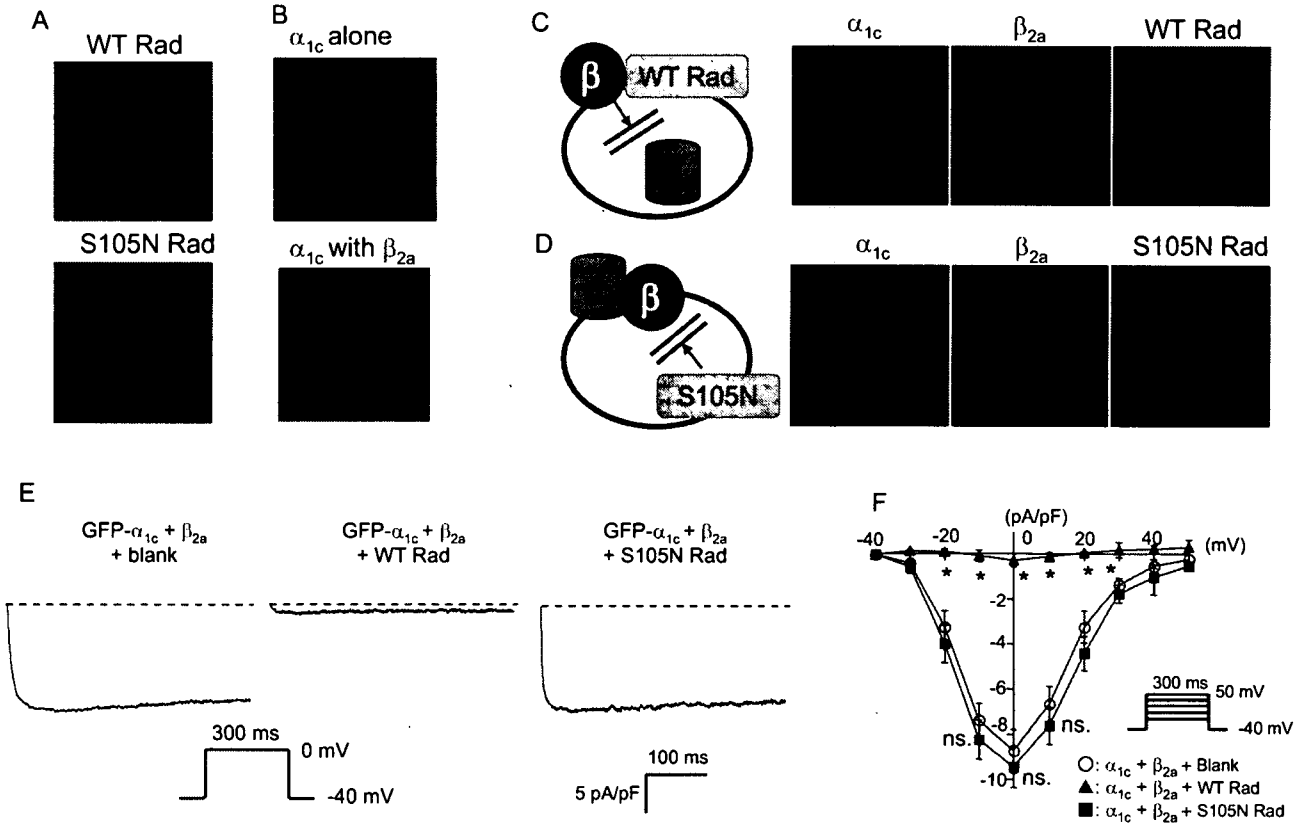

Figure 2. Rad regulates L-type Ca^{2+} channel function via α subunit trafficking to plasma membrane. A, Localization of WT Rad and S105N Rad in HEK293 cells. B, Localization of Ca^{2+} channel α_{1c} subunits in HEK293 cells, when expressed with or without β_{2a} subunit. C and D, Subcellular localization of GFP-α_{1c} subunit (green) and Flag-tagged β_{2a} subunit (blue) in a cell coexpressing hemagglutinin-tagged WT Rad or S105N Rad (red). The localizations of each subunit are depicted diagrammatically on the left. E, Representative Ba^{2+} current traces in HEK293 cells transiently cotransfected with GFP-α_{1c} subunit, β_{2a} subunit, and blank, WT Rad, or S105N Rad. Dashed lines indicate 0 current. F, Current/voltage relationships of Ba^{2+} currents in HEK293 cells cotransfected with GFP-α_{1c} subunit, β_{2a} subunit, and blank (n=7), GFP-α_{1c} subunit, β_{2a} subunit, and WT Rad (n=4), or GFP-α_{1c} subunit, β_{2a} subunit, and S105N Rad (n=6). ns indicates not significant vs control, *P<0.01 vs control.

subunits showed an interaction with WT Rad (Figure 1B), but no interaction with S105N Rad was detected. Because S105N Rad, which could bind GDP but not GTP, is known to function as a dominant negative mutant in the regulation of neointimal formation after vascular injury,[6] we examined whether S105N Rad showed dominant negative inhibition of the interaction between WT Rad and β subunits. A plasmid encoding S105N Rad fused with Myc tag at its N terminus was cotransfected with WT Rad and β_{2a}-subunit plasmids into HEK293 cells. As shown in Figure 1C, Myc-tagged S105N Rad suppressed the interaction between WT Rad and β_{2a} subunits in a dose-dependent manner, indicating that S105N Rad did function as a dominant negative mutant for the interaction between WT Rad and β_{2a} subunits.

Based on these results, we next studied whether the interaction between Rad and the β subunit affected the trafficking of Ca^{2+} channel α subunit to the plasma membrane. To do this, green fluorescent protein (GFP)-fused $Ca_v1.2$ (cardiac α_{1c} subunit) and β_{2a} subunit were coimmunostained with WT Rad or S105N Rad in HEK293 cells and visualized by confocal microscopy. Both WT Rad and S105N Rad were localized at the plasma membrane, when expressed alone (Figure 2A). Although individually expressed α_{1c} subunit was localized mainly in the cytoplasm (Figure 2B), cotransfection with β_{2a} subunits resulted in the translocation of α_{1c} subunits from the cytoplasm to plasma membrane, confirming that the β subunit plays a chaperon-like role with the α_{1c} subunit (Figure 2B). When WT Rad was expressed together with both the α_{1c} and β_{2a} subunits, the α_{1c} subunit showed a cytoplasmic distribution, whereas WT Rad and the β_{2a} subunit were still colocalized at the plasma membrane, indicating that WT Rad disrupted the binding of α_{1c} subunit to β_{2a} subunit (Figure 2C). In contrast, S105N Rad did not affect the localization of the α_{1c} and β_{2a} subunits (Figure 2D). These results indicated that the interaction between Rad and the β subunit regulated the trafficking of the α_{1c} subunit to the plasma membrane.

To examine whether Rad regulates the function of L-type Ca^{2+} channels, we recorded Ba^{2+} currents in HEK293 cells using the whole-cell patch clamp technique. Currents conducted by L-type Ca^{2+} channels were recorded with 4 mmol/L Ba^{2+} in the external solution as a charge carrier. The currents in cells in which S105N Rad was coexpressed with GFP-α_{1c} subunit and β_{2a} subunit were similar to those in control cells (average current densities for GFP-α_{1c} subunit, β_{2a} subunit, and S105N Rad: 9.4±0.9 pA/pF [n=6]; for GFP-α_{1c} subunit, β_{2a} subunit, and blank: 8.8±0.9 pA/pF [n=7]; not significant), whereas in cells expressing the GFP-α_{1c} subunit, β_{2a}

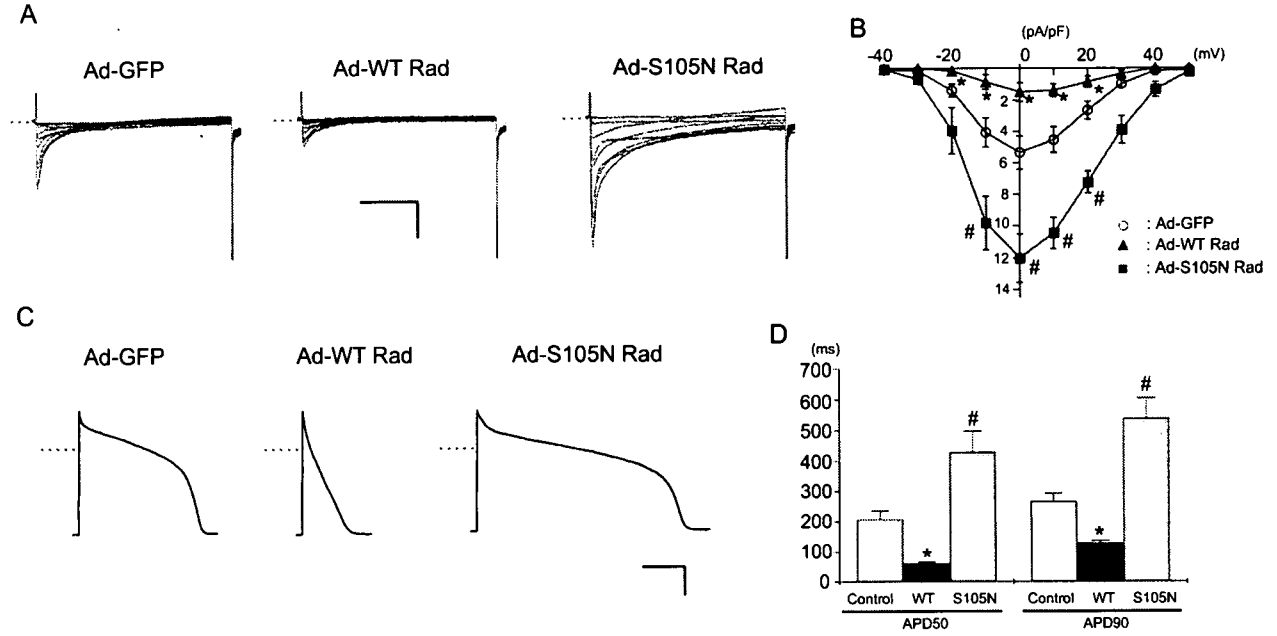

Figure 3. Effects of Rad on L-type Ca^{2+} current and action potential configuration in guinea pig ventricular cardiomyocytes. A, Representative $I_{Ca,L}$ traces in an Ad-GFP–transduced (control) cell, an Ad-WT Rad–transduced cell, and an Ad-S105N Rad–transduced cell. Dashed lines indicate 0 current. B, Current/voltage relationships of $I_{Ca,L}$ in control (n=8), Ad-WT Rad–transduced (n=6), and Ad-S105N Rad–transduced (n=7) cells. #$P<0.05$ vs control, *$P<0.01$ vs control. C. Representative action potential traces in a control cell, an Ad-WT Rad–transduced cell, and an Ad-S105N Rad–transduced cell. Dashed lines indicate 0 mV. D, Pooled data for APD in control (n=8), Ad-WT Rad–transduced (n=5), and Ad-S105N Rad–transduced (n=6) cells. #$P<0.05$ vs control, *$P<0.01$ vs control.

subunit, and WT Rad, the currents were very small (0.20±0.03 pA/pF [n=5] versus control; $P<0.01$), and similar to those in cells expressing GFP-α_{1c} subunit alone (0.19±0.04 pA/pF [n=5]), indicating the association of WT Rad-mediated suppression with the β subunit (Figure 2E and 2F). These results confirmed that WT Rad dramatically suppressed the function of the L-type Ca^{2+} channel, whereas S105N Rad did not.

Rad Regulates $I_{Ca,L}$ via Inhibition of α subunit trafficking to Plasma Membrane in Guinea Pig Ventricular Cardiomyocytes

To investigate the physiological role of Rad in the heart, we transduced adenovirus (Ad) encoding WT Rad or S105N Rad into guinea pig ventricular cardiomyocytes and recorded $I_{Ca,L}$ using the whole-cell patch clamp technique. Interestingly, the peak $I_{Ca,L}$ was larger in the cells overexpressing S105N Rad than in controls (12.0±1.5 pA/pF at 0 mV [n=7] in Ad-S105N Rad–transduced cells versus 5.4±1.0 pA/pF at 0 mV [n=8] in Ad-GFP transduced controls: $P<0.05$), whereas $I_{Ca,L}$ was dramatically smaller in cells overexpressing WT Rad (1.4±0.1 pA/pF at 0 mV [n=6] in Ad-WT Rad–transduced cells versus control; $P<0.01$) (Figure 3A and 3B). Because S105N Rad itself does not affect the $I_{Ca,L}$, as shown in Figure 2F, enhancement of $I_{Ca,L}$ by S105N Rad in cardiomyocytes might be attributable to the dominant negative suppression of endogenous Rad activity. Because the L-type Ca^{2+} channel contributes to the ion influx and plateau phase of the cardiac action potential, we investigated whether Rad-mediated regulation of $I_{Ca,L}$ might affect the action potential in heart cells. Action potentials were recorded in guinea pig ventricular cells transduced with Ad-GFP (control), Ad-WT Rad, and Ad-S105N Rad. As expected, overexpression of WT Rad resulted in a dramatic shortening of the action potential duration (APD) and abolished the robust action potential plateau (APD_{90} 128±7.76 ms [n=5] in Ad-WT Rad–transduced cells versus 267±26.3 ms [n=8] in Ad-GFP–transduced control cells; $P<0.01$), whereas S105N Rad significantly prolonged the APD without changing the action potential configuration (538±70.0 ms [n=6] in Ad-S105N Rad–transduced cells versus control; $P<0.01$) (Figure 3C and 3D).

To investigate the mechanisms of Rad-mediated regulation of $I_{Ca,L}$ in native guinea pig cardiomyocytes, we performed cell fractionation and used Western blot analysis to quantify the expression of α_{1c} subunit in the plasma membrane of cells after 24 hours in culture. The amount of α_{1c} subunit protein extracted from the membrane fraction was significantly lower in Ad-WT Rad–transduced cells than in Ad-GFP–transduced control cells, whereas the overexpression of S105N Rad resulted in a significantly greater extraction of α_{1c} subunit protein from the membrane fraction (Figure 4). These findings show that dominant negative suppression of endogenous Rad by S105N Rad increased Ca^{2+} channel expression at the plasma membrane, thereby implicating endogenous Rad in the regulation of cardiac L-type Ca^{2+} channel expression in the physiological context.

In Vivo Phenotype of Dominant Negative Suppression of Rad in Mouse Heart

To investigate the physiological role of endogenous Rad in vivo, we took advantage of the dominant negative mutant Rad

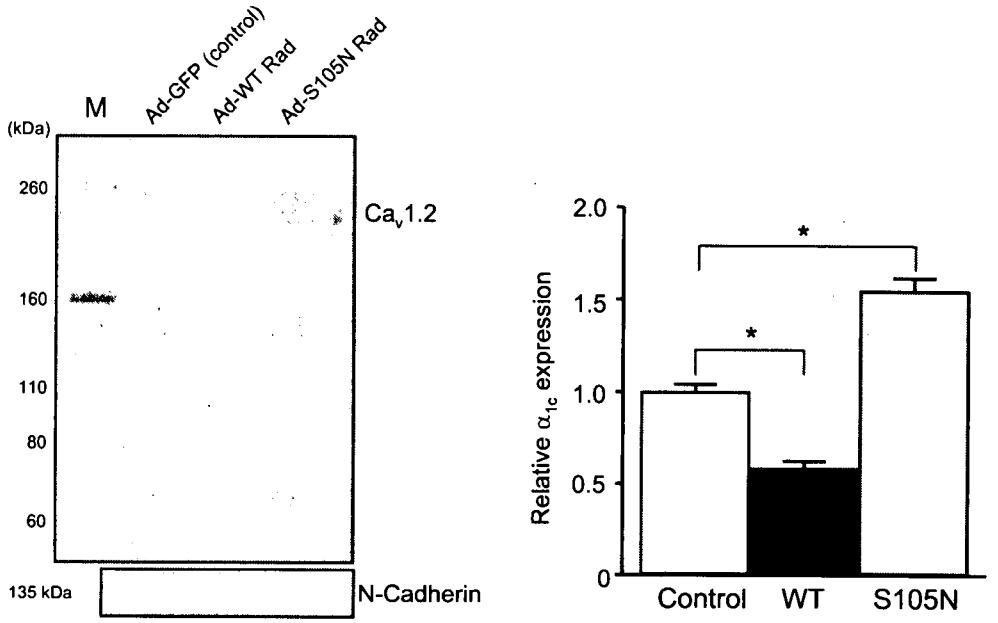

Figure 4. Rad modulates L-type Ca^{2+} channel membrane expression in guinea pig ventricular cardiomyocytes. Quantitative Western blot analysis comparing α_{1c} subunit protein extracted from plasma membranes of cardiomyocytes transduced with Ad-GFP (control), Ad-WT Rad, or Ad-S105N Rad after 24 hours in culture. N-Cadherin was used as an internal control for the membrane protein fraction. M indicates molecular size markers. Data are from 5 independent experiments. *$P<0.05$ vs control.

to engineer an in vivo model of Rad disruption, obtained by overexpressing the S105N Rad under the control of the α-myosin heavy chain promoter. In transgenic (TG) mice aged 12 weeks, the total Rad protein expression in whole heart was 6 times greater than in their WT littermates (Figure 5A), indicating that the expression level of S105N Rad was approximately 5 times that of endogenous Rad. This level of exogenous S105N Rad expression in TG mice should have been sufficient to suppress the endogenous Rad/β subunit interaction, as shown in Figure 1B. Thus, we performed coimmunoprecipitation assays to confirm the effect of S105N Rad overexpression on the endogenous Rad/β subunit interaction in whole hearts. As shown in Figure 5B, the total amount of Rad that bound to the β subunits was much less in S105N TG mouse heart than that in WT mouse heart. Furthermore, we used Western blot analysis to compare α_{1c} protein expression in the plasma membranes of S105N Rad TG and WT mice. The α_{1c} protein expression was significantly greater in S105N Rad TG mice than WT mice, supporting the proposition that dominant negative suppres-

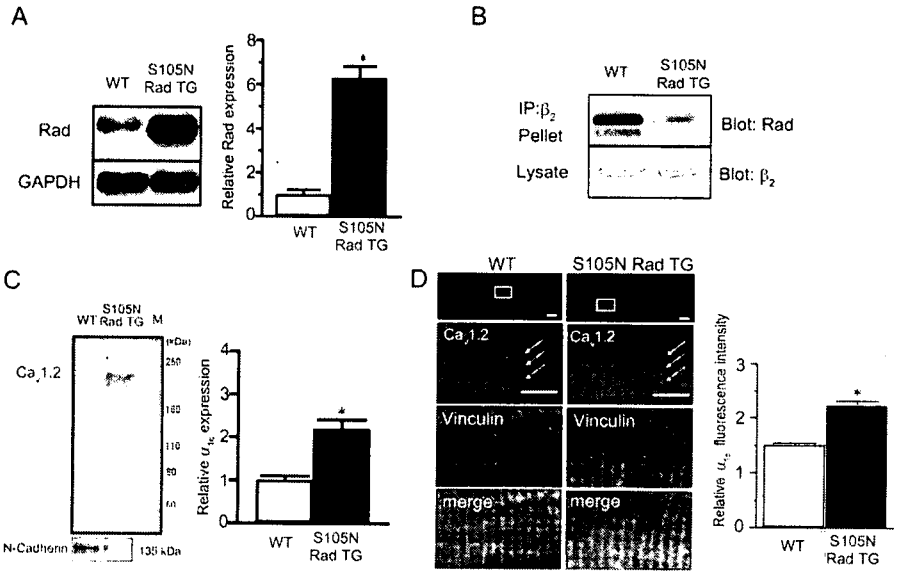

Figure 5. S105N Rad suppresses the in vivo interaction between Rad and β subunit in the heart. A, Western blot analysis comparing total Rad protein level in cardiac muscle from WT and S105N Rad TG mice. Data are from 5 WT and 5 S105N Rad TG mice. *$P<0.05$ vs WT. B, In vivo interaction between Rad and β subunit in the heart. Lysates from whole heart were coimmunoprecipitated with anti-β_2 subunit antibody, and associated Rad proteins were detected by Western blotting. C, Western blot of cardiac α_{1c} subunit protein in the membrane fraction from WT and S105N Rad TG mouse hearts. N-Cadherin was used as an internal control for the membrane fraction. M indicates molecular size markers. Data are from 5 WT and 5 S105N Rad TG mice. *$P<0.05$ vs WT. D, Immunohistochemical analysis of α_{1c} subunits in WT and S105N Rad TG ventricular cardiomyocytes. The white squares in the upper panels indicate the regions shown at higher magnification below. Vinculin was used as a T-tubule marker. Scale bar=10 μm. Pooled data for relative α_{1c} mean fluorescence in WT (n=10) and S105N Rad TG mouse cardiomyocytes (n=10).

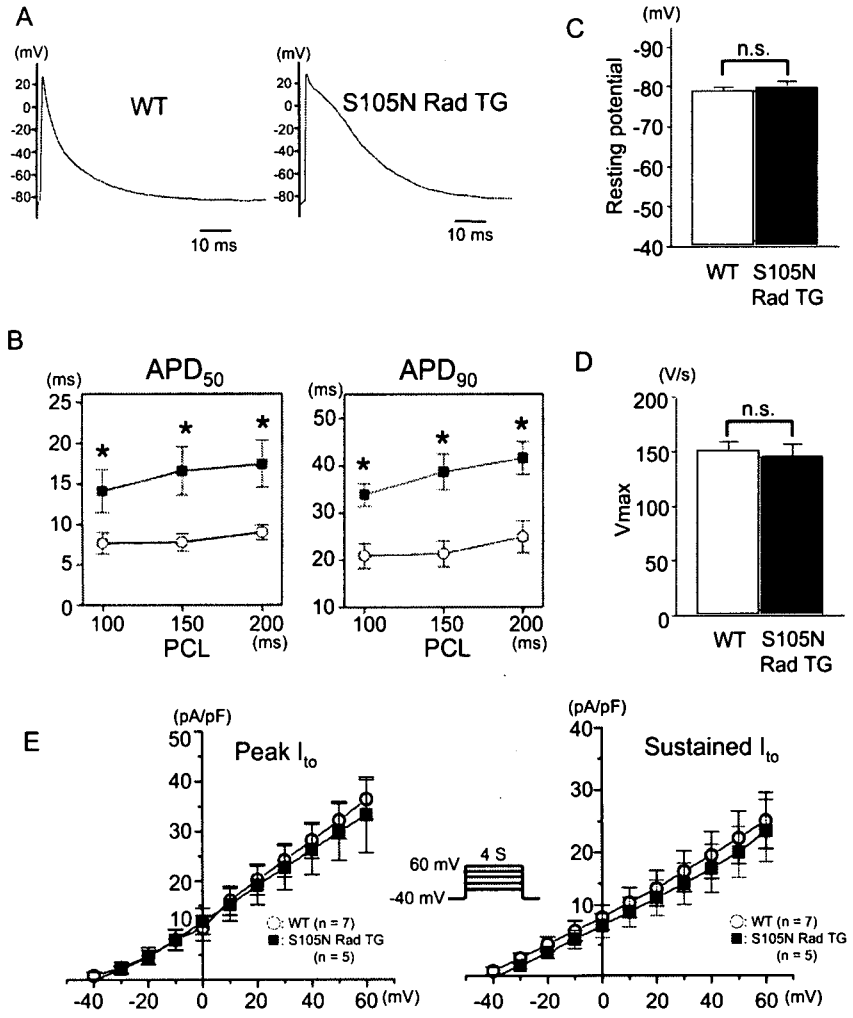

Figure 6. A, Representative action potential traces recorded from papillary muscle samples from WT and S105N Rad TG mice. B, Effects of pacing cycle length (PCL) on APD at 50% (APD_{50}) and 90% (APD_{90}) repolarization in WT (filled circles; n=8) and S105N Rad TG mice (filled squares; n=8). *$P<0.05$ vs WT. C, Pooled data for resting membrane potential recorded from papillary muscles of WT (n=8) and S105N Rad TG mice (n=8). D, Pooled data for V_{max} recorded from papillary muscles of WT (n=8) and S105N Rad TG mice (n=8). E, Current/voltage relationships of I_{to} peak and sustained currents in WT (n=8) and S105N Rad-TG mouse cells (n=5). ns indicates not significant vs WT cells.

sion of Rad facilitates α_{1c} subunit expression at the plasma membrane (Figure 5C). Accordingly, immunohistological analysis revealed that the T tubules of ventricular cardiomyocytes isolated from S105N Rad TG mouse hearts were more intensely immunoreactive for α_{1c} subunits than those of WT mice (Figure 5D). The relative mean fluorescence of α_{1c} subunits in the T-tubule areas to that in non–T-tubule area (between T tubules) were significantly greater in the S105N Rad TG mouse cells than in the WT mouse cells, indicating that S105N Rad facilitated the α_{1c} subunit trafficking to the T tubules in cardiomyocytes (Figure 5D).

Next, action potentials were recorded from left ventricular papillary muscles using conventional microelectrode techniques. The APD was measured at 3 different pacing cycle lengths (100 ms, 150 ms, and 200 ms). As shown in Figure 6A, the APD was prolonged, and a subtle plateau phase was observed in S105N Rad TG mice. Consistent with the in vitro data in guinea pig cells, the APD_{50} and APD_{90} were both longer in S105N Rad TG mice than in WT mice at each pacing cycle length (Figure 6B; APD_{90} at 100 ms pacing cycle length, 33.9±2.5 ms [n=8] in S105N TG mice, versus 20.9±2.6 ms [n=8] in WT mice; $P<0.05$). There were no significant differences in resting membrane potential or V_{max} between WT and TG mice (Figure 6C and 6D), suggesting that dominant negative suppression of Rad did not affect the inward rectifying K^+ currents and Na^+ currents. We also examined the transient outward potassium current (I_{to}), which mainly affects repolarization in the mouse action potential. There were no significant differences between the WT and S105N Rad TG mice in either peak or sustained I_{to} current densities, implying that Rad did not affect I_{to} function (Figure 6E).

As expected from the APD data, surface electrocardiograms showed QT prolongation in S105N Rad TG mice compared with WT mice (Figure 7A). Both QT and QTc intervals in S105N Rad TG mice were significantly longer than those in WT mice (QTc, 60.1±3.0 ms [n=8] in S105N Rad TG mice, versus 47.3±3.3 ms [n=8] in WT mice; $P<0.05$; Figure 7B). No significant differences were detected in other ECG parameters, such as RR, PR, and QRS intervals, as described in Table I in the online data supplement. Given the importance of QT prolongation as a cause of lethal ventricular arrhythmias, we investigated whether the dominant negative suppression of endogenous Rad activity produced arrhythmias in S105N Rad TG mice. In vivo ECGs were recorded from freely moving mice for 24 hours. No arrhythmias were observed in the recordings from WT mice (n=8). In contrast, among the TG mice (n=8), we recorded

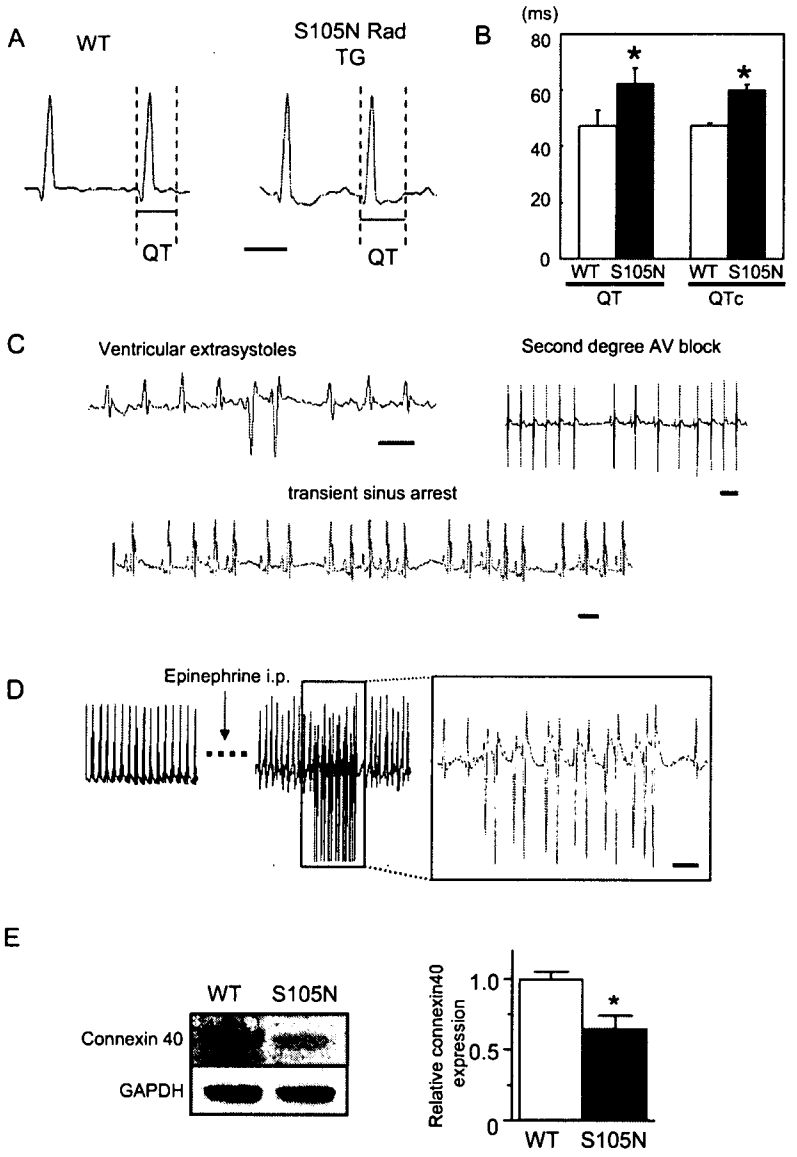

Figure 7. Characteristics of ECGs in S105N Rad TG mice. A, ECG recordings from a WT and a S105N Rad TG mouse. Scale bar=50 ms. B, Pooled data for QT and QTc intervals recorded from WT (n=8) and S105N Rad TG mice (n=8). *$P<0.05$ vs WT. C, Telemetric ECG recording from a freely moving S105N Rad TG mouse. Second degree atrioventricular (AV) block, transient sinus arrest, and frequent ventricular extrasystoles were recorded in S105N Rad TG mice during normal activity. Scale bar=100 ms. D, Nonsustained ventricular tachycardia was induced by intraperitoneal injection of epinephrine in S105N Rad TG mice. Scale bar=100 ms. E, Western blot analysis comparing connexin40 protein level in atrial tissues from WT and S105N Rad TG mice. Data are from 4 WT and 4 S105N Rad TG mice. *$P<0.05$ vs WT.

transient sinus arrest and second-degree atrioventricular block in 6 mice each, and ventricular extrasystoles in 5 mice (Figure 7C). In some patients with long QT syndrome, fatal ventricular arrhythmias occur under physical exertion and emotional stress.[17,18] To mimic these circumstances, we injected epinephrine (2 mg/kg) into the peritoneum of S105N Rad TG mice (n=8) and WT mice (n=8). Under the epinephrine loading, nonsustained ventricular tachycardia was induced in 3 of the TG mice (Figure 7D), and consecutive ventricular extrasystoles were more frequently observed (7 TG mice), although no ventricular arrhythmias were observed in WT mice (see supplemental Table II).

Because the increase in $I_{Ca,L}$ should facilitate nodal conduction, the abnormal nodal function observed in TG mice seemed anomalous. Rad is also known to suppress the Rho signaling pathway by direct interaction with its substrate, ROCK.[3] Furthermore, disruption of Rho signaling results in progressive atrioventricular conduction defects, probably attributable to a dramatic decrease of connexin40.[19,20] We examined the atrial expression of connexin40 in mouse hearts by Western blot analysis. As expected, connexin40 expression was significantly lower in S105N Rad TG mice than WT mice (Figure 7E).

Discussion

The major finding of this study was that dominant negative suppression of endogenous Rad in the heart resulted in an increase in $I_{Ca,L}$, via upregulation of L-type Ca^{2+} channel expression at the plasma membrane. Using a transgenic approach for cardiac-specific inhibition of Rad by expressing the dominant negative form of Rad (S105N), the present study provides important new insights into the physiological function of Rad in regulating cardiac electrophysiology. Although mouse echocardiography showed no significant changes in cardiac size or function in transgenic animals at 12 weeks of age (supplemental Figure I), the phenotype of the transgenic animals comprised a prolonged QT interval, nodal dysfunction, and extrasystoles. These ECG phenotypes were

accompanied by prolonged APDs and enhanced $I_{Ca,L}$, which were attributable to the upregulation of L-type Ca^{2+} channels in T tubules. Under baseline conditions, TG mice displayed ventricular extrasystoles but no ventricular tachycardia. Furthermore, epinephrine administration exacerbated the ventricular arrhythmias in TG mice but did not induce arrhythmias in WT mice. These data indicate that the Rad signaling pathway plays an important role in cardiac antiarrhythmia via the strong suppression of $I_{Ca,L}$.

We did not predict any nodal dysfunction in TG mice because an increase of $I_{Ca,L}$ would be expected to facilitate nodal conduction. The induction of nodal dysfunction was probably attributable, at least in part, to the reduction of connexin40 expression in TG mice. Previous studies have shown that Rad binds directly to ROCK, resulting in the inhibition of Rho/ROCK signaling pathways,[3,6] which regulates the connexin40 expression in mouse hearts.[19] The GST pull-down assays revealed that S105N Rad, as well as WT Rad, could physically interact with ROCK (data not shown). This implies that overexpression of S105N Rad in TG mice may have led to a decrease of connexin40 expression via suppression of the Rho signaling pathways. Furthermore, this inhibitory effect of Rad on Rho pathways was likely to have been especially strong in the heart because Rad binds to ROCK2, which is highly expressed in the heart, whereas the other isoform (ROCK1) is preferentially expressed in noncardiac tissues such as lung, liver, spleen, kidney, and testis.[21] This distinct tissue-specific expression of ROCK isoforms might explain the opposite effects of Gem and Rad on nodal conduction because Gem predominantly binds to ROCK1.[3] However, further studies are needed to test this hypothesis.

One major cause of mortality in patients with diabetes mellitus is diabetic cardiomyopathy, which occurs independently from diabetes-mediated vascular complications. Pereira et al[22] reported that the systolic dysfunction of type 2 diabetic mice is partly attributable to a reduction of $I_{Ca,L}$, implicating Rad-mediated Ca^{2+} channel regulation as a possible factor in diabetic cardiomyopathy. Furthermore, diabetic cardiomyopathy is characterized by electrical remodeling, metabolic remodeling with malignant biochemical processes, and anatomical remodeling with progressive loss of cardiomyocytes.[23] The abnormal prolongation of QT interval is the most prominent electrical remodeling that occurs in diabetic hearts. QT prolongation is a significant predictor of mortality in diabetes patients because it is associated with an increased risk of sudden cardiac death caused by lethal ventricular arrhythmias.[24] One of the mechanisms for QT prolongation in diabetes mellitus is depression of multiple ion currents including the transient outward current, $I_{Ca,L}$, and the delayed rectifier K^+ current.[22,25] Given that Rad mRNA is upregulated in type 2 diabetes patients[2] and Rad protein expression in diabetic mouse heart is upregulated relative to WT mice (data not shown), Rad-mediated regulation of $I_{Ca,L}$ might be involved in the electrophysiological remodeling in diabetic cardiomyopathy. Dominant negative suppression of Rad led to QT prolongation and induction of arrhythmias even in the nondiabetic mice used in this study. Considering these experimental and clinical data, it is plausible that upregulation of Rad in diabetic patients might function as a negative regulator to counteract QT prolongation by compensating for the decreased outward K^+ currents with downregulation of $I_{Ca,L}$. If so, the preservation of Rad function might be a potential strategy for the prevention of lethal ventricular arrhythmias in diabetic cardiomyopathy.

Our data clearly demonstrated that Rad regulated the trafficking of Ca^{2+} channel α subunit in both heterologous systems and cardiomyocytes. However, the precise mechanisms of RGK protein-mediated modulation of L-type Ca^{2+} channels remain to be clarified. Consistent with our data, Beguin et al[9] showed that inhibition of $I_{Ca,L}$ by another RGK protein, Gem, is attributable to the decreased expression of α subunits in the plasma membrane. However, in our study, the complete inhibition of $I_{Ca,L}$ 24 hours after transduction of WT Rad in guinea pig cells could not be explained solely by the suppression of α subunit trafficking to the plasma membrane because our Western blot data still detected a small amount of Ca^{2+} channel expression in the T tubules. These channels may have remained because the turnover of L-type Ca^{2+} channels in the plasma membrane is 36 to 48 hours[26]; thus a 24 hour culture period might not be sufficient for the complete degradation of preexisting channels. Therefore, other mechanisms for suppression of $I_{Ca,L}$ by Rad, unrelated to trafficking, are also likely to be involved. One possibility is the direct inhibition of L-type Ca^{2+} channels by association of Rad with channel subunits. Rem2 has recently been shown to almost completely suppress $I_{Ca,L}$ without altering channel expression at the plasma membrane,[27,28] which supports this hypothesis. The possibility remains that Rad may regulate the expression of other RGK proteins, which in turn alter L-type Ca^{2+} channel function. However, the expression level of Rem protein did not change with overexpression of Rad (data not shown), which leads us to conclude that Rem is not associated with the Rad-mediated regulation of the L-type Ca^{2+} channel. Further studies are required to identify the multiple mechanisms involved in regulation of the L-type Ca^{2+} channel by Rad.

In summary, dominant negative suppression of Rad in the heart induced QT prolongation and ventricular arrhythmias, caused by the augmentation of $I_{Ca,L}$. The finding that Rad regulates L-type Ca^{2+} channel function in the heart suggests that the Rad-associated signaling pathway may play a role in arrhythmogenesis in diverse cardiac diseases.

Acknowledgments

We thank Dr Shunichiro Miyoshi and Dr Yoko Hagiwara for useful technical advice.

Sources of Funding

This study was supported by research grants from the Ministry of Education, Science and Culture, Japan (to M.M., T.A., and K.F.); from Keio Gijuku Academic Developmental Funds (to M.M.); from the Program for Promotion of Fundamental Studies in Health Sciences of the National Institute of Biomedical Innovation (to K.F.); and from health sciences research grants from the Ministry of Health, Labour and Welfare, Japan (H18-Research on Human Genome-002 to S.O.).

Disclosures

None.

References

1. Kelly K. The RGK family: a regulatory tail of small GTP-binding proteins. *Trends Cell Biol.* 2005;15:640–643.
2. Reynet C, Kahn CR. Rad: a member of the Ras family overexpressed in muscle of type II diabetic humans. *Science.* 1993;262:1441–1444.
3. Ward Y, Yap SF, Ravichandran V, Matsumura F, Ito M, Spinelli B, Kelly K. The GTP binding proteins Gem and Rad are negative regulators of the Rho-Rho kinase pathway. *J Cell Biol.* 2002;157:291–302.
4. Moyers JS, Bilan PJ, Zhu J, Kahn CR. Rad and Rad-related GTPases interact with calmodulin and calmodulin-dependent protein kinase II. *J Biol Chem.* 1997;272:11832–11839.
5. Beguin P, Mahalakshmi RN, Nagashima K, Cher DH, Kuwamura N, Yamada Y, Seino Y, Hunziker W. Roles of 14-3-3 and calmodulin binding in subcellular localization and function of the small G-protein Rem2. *Biochem J.* 2005;390:67–75.
6. Fu M, Zhang J, Tseng YH, Cui T, Zhu X, Xiao Y, Mou Y, De Leon H, Chang MM, Hamamori Y, Kahn CR, Chen YE. Rad GTPase attenuates vascular lesion formation by inhibition of vascular smooth muscle cell migration. *Circulation.* 2005;111:1071–1077.
7. Ilany J, Bilan PJ, Kapur S, Caldwell JS, Patti ME, Marette A, Kahn CR. Overexpression of Rad in muscle worsens diet-induced insulin resistance and glucose intolerance and lowers plasma triglyceride level. *Proc Natl Acad Sci U S A.* 2006;103:4481–4486.
8. Finlin BS, Mosley AL, Crump SM, Correll RN, Ozcan S, Satin J, Andres DA. Regulation of L-type Ca^{2+} channel activity and insulin secretion by the Rem2 GTPase. *J Biol Chem.* 2005;280:41864–41871.
9. Beguin P, Nagashima K, Gonoi T, Shibasaki T, Takahashi K, Kashima Y, Ozaki N, Geering K, Iwanaga T, Seino S. Regulation of Ca^{2+} channel expression at the cell surface by the small G-protein kir/Gem. *Nature.* 2001;411:701–706.
10. Murata M, Cingolani E, McDonald AD, Donahue JK, Marban E. Creation of a genetic calcium channel blocker by targeted gem gene transfer in the heart. *Circ Res.* 2004;95:398–405.
11. Sasaki T, Shibasaki T, Beguin P, Nagashima K, Miyazaki M, Seino S. Direct inhibition of the interaction between alpha-interaction domain and beta-interaction domain of voltage-dependent Ca^{2+} channels by Gem. *J Biol Chem.* 2005;280:9308–9312.
12. Mitra R, Morad M. Two types of calcium channels in guinea pig ventricular myocytes. *Proc Natl Acad Sci U S A.* 1986;83:5340–5344.
13. Hoppe UC, Johns DC, Marban E, O'Rourke B. Manipulation of cellular excitability by cell fusion: effects of rapid introduction of transient outward K^+ current on the guinea pig action potential. *Circ Res.* 1999; 84:964–972.
14. Subramaniam A, Jones WK, Gulick J, Wert S, Neumann J, Robbins J. Tissue-specific regulation of the alpha-myosin heavy chain gene promoter in transgenic mice. *J Biol Chem.* 1991;266:24613–24620.
15. Beguin P, Mahalakshmi RN, Nagashima K, Cher DH, Ikeda H, Yamada Y, Seino Y, Hunziker W. Nuclear sequestration of beta-subunits by Rad and Rem is controlled by 14-3-3 and calmodulin and reveals a novel mechanism for Ca^{2+} channel regulation. *J Mol Biol.* 2006;355:34–46.
16. Finlin BS, Crump SM, Satin J, Andres DA. Regulation of voltage-gated calcium channel activity by the Rem and Rad GTPases. *Proc Natl Acad Sci U S A.* 2003;100:14469–14474.
17. Shimizu W, Noda T, Takaki H, Kurita T, Nagaya N, Satomi K, Suyama K, Aihara N, Kamakura S, Sunagawa K, Echigo S, Nakamura K, Ohe T, Towbin JA, Napolitano C, Priori SG. Epinephrine unmasks latent mutation carriers with LQT1 form of congenital long-QT syndrome. *J Am Coll Cardiol.* 2003;41:633–642.
18. Paavonen KJ, Swan H, Piippo K, Hokkanen L, Laitinen P, Viitasalo M, Toivonen L, Kontula K. Response of the QT interval to mental and physical stress in types LQT1 and LQT2 of the long QT syndrome. *Heart.* 2001;86:39–44.
19. Wei L, Taffet GE, Khoury DS, Bo J, Li Y, Yatani A, Delaughter MC, Klevitsky R, Hewett TE, Robbins J, Michael LH, Schneider MD, Entman ML, Schwartz RJ. Disruption of Rho signaling results in progressive atrioventricular conduction defects while ventricular function remains preserved. *FASEB J.* 2004;18:857–859.
20. Simon AM, Goodenough DA, Paul DL. Mice lacking connexin40 have cardiac conduction abnormalities characteristic of atrioventricular block and bundle branch block. *Curr Biol.* 1998;8:295–298.
21. Noma K, Oyama N, Liao JK. Physiological role of ROCKs in the cardiovascular system. *Am J Physiol Cell Physiol.* 2006;290:C661–C668.
22. Pereira L, Matthes J, Schuster I, Valdivia HH, Herzig S, Richard S, Gomez AM. Mechanisms of $[Ca^{2+}]i$ transient decrease in cardiomyopathy of db/db type 2 diabetic mice. *Diabetes.* 2006;55:608–615.
23. Casis O, Echevarria E. Diabetic cardiomyopathy: electromechanical cellular alterations. *Curr Vasc Pharmacol.* 2004;2:237–248.
24. Rossing P, Breum L, Major-Pedersen A, Sato A, Winding H, Pietersen A, Kastrup J, Parving HH. Prolonged QTc interval predicts mortality in patients with type 1 diabetes mellitus. *Diabet Med.* 2001;18:199–205.
25. Wang DW, Kiyosue T, Shigematsu S, Arita M. Abnormalities of K^+ and Ca^{2+} currents in ventricular myocytes from rats with chronic diabetes. *Am J Physiol.* 1995;269:H1288–H1296.
26. Moss FJ, Viard P, Davies A, Bertaso F, Page KM, Graham A, Canti C, Plumpton M, Plumpton C, Clare JJ, Dolphin AC. The novel product of a five-exon stargazin-related gene abolishes $Ca_v2.2$ calcium channel expression. *EMBO J.* 2002;21:1514–1523.
27. Chen H, Puhl HL 3rd, Niu SL, Mitchell DC, Ikeda SR. Expression of Rem2, an RGK family small GTPase, reduces N-type calcium current without affecting channel surface density. *J Neurosci.* 2005;25: 9762–9772.
28. Finlin BS, Correll RN, Pang C, Crump SM, Satin J, Andres DA. Analysis of the complex between Ca^{2+} channel β-subunit and the Rem GTPase. *J Biol Chem.* 2006;281:23557–23566.

nature medicine

Sema3a maintains normal heart rhythm through sympathetic innervation patterning

Masaki Ieda[1,2], Hideaki Kanazawa[1,2], Kensuke Kimura[1], Fumiyuki Hattori[1], Yasuyo Ieda[1], Masahiko Taniguchi[3], Jong-Kook Lee[4], Keisuke Matsumura[1,2], Yuichi Tomita[1], Shunichiro Miyoshi[2], Kouji Shimoda[5], Shinji Makino[1], Motoaki Sano[1], Itsuo Kodama[4], Satoshi Ogawa[2] & Keiichi Fukuda[1]

Sympathetic innervation is critical for effective cardiac function. However, the developmental and regulatory mechanisms determining the density and patterning of cardiac sympathetic innervation remain unclear, as does the role of this innervation in arrhythmogenesis. Here we show that a neural chemorepellent, Sema3a, establishes cardiac sympathetic innervation patterning. Sema3a is abundantly expressed in the trabecular layer in early-stage embryos but is restricted to Purkinje fibers after birth, forming an epicardial-to-endocardial transmural sympathetic innervation patterning. *Sema3a*$^{-/-}$ mice lacked a cardiac sympathetic innervation gradient and exhibited stellate ganglia malformation, which led to marked sinus bradycardia due to sympathetic dysfunction. Cardiac-specific overexpression of *Sema3a* in transgenic mice (*SemaTG*) was associated with reduced sympathetic innervation and attenuation of the epicardial-to-endocardial innervation gradient. *SemaTG* mice demonstrated sudden death and susceptibility to ventricular tachycardia, due to catecholamine supersensitivity and prolongation of the action potential duration. We conclude that appropriate cardiac Sema3a expression is needed for sympathetic innervation patterning and is critical for heart rate control.

Cardiac tissues are extensively innervated by autonomic nerves. The cardiac sympathetic nerves extend from the sympathetic neurons in stellate ganglia, which reside bilateral to the vertebrae. Previous studies have established regional differences in the sympathetic innervation of the heart in larger mammals[1,2]. Sympathetic nerve fibers project from the base of the heart into the myocardium and are located predominantly in the subepicardium in the ventricle[3,4]. The central conduction system, including the sinoatrial node, the atrioventricular node and the His bundle, is abundantly innervated as compared with the working myocardium[1,4–6]. The sympathetic nervous system augments cardiac performance by increasing heart rate, conduction velocity, myocardial contraction, and relaxation. Accordingly, unbalanced neural activation or suppression might trigger lethal arrhythmia in diseased hearts[7–10]. These findings have demonstrated that sympathetic innervation patterning is critical for effective cardiac performance; however, little is known about the developmental and regulatory mechanisms underlying cardiac sympathetic innervation patterning. Moreover, the consequence of its disruption remains unknown.

We and others have reported that nerve growth factor (NGF), a member of the neurotrophin family, is required for sympathetic axon growth and innervation in the heart[11,12]. However, the neural chemorepellent that induces growth cone collapse and repels sympathetic axons in the heart has not been identified. Sema3a is a class 3 secreted semaphorin and a potent neural chemorepellent for sensory and sympathetic axons[13–15]. Targeted inactivation of *Sema3a* disrupts neural patterning and projections, indicating the importance of Sema3a signaling for directional guidance of nerve fibers[16,17]. It remains unknown, however, whether cardiomyocytes produce Sema3a, and, if so, whether this protein affects sympathetic neural patterning and cardiac performance. Here we demonstrate the expression pattern of Sema3a in developing hearts and its critical roles in cardiac sympathetic innervation patterning and arrhythmia, using various gene-modified mouse models.

RESULTS

Sympathetic nerve distribution in mouse heart

We first analyzed the distribution of cardiac sympathetic nerves in adult mouse hearts at postnatal day (P) 42 by immunostaining with an antibody to tyrosine hydroxylase, a marker of sympathetic nerves. Tyrosine hydroxylase–immunopositive (TH^+) nerves were most abundant in the sinoatrial node, the atrioventricular node and the His bundle, as indicated by acetyl cholinesterase (AChE) activity staining (refs. 18,19 and **Fig. 1a**). In contrast, TH^+ nerves in Purkinje

[1]Department of Regenerative Medicine and Advanced Cardiac Therapeutics, Keio University School of Medicine, 35 Shinanomachi, Shinjuku-ku, Tokyo 160-8582, Japan. [2]Cardiology Division, Department of Medicine, Keio University School of Medicine, 35 Shinanomachi, Shinjuku-ku, Tokyo 160-8582, Japan. [3]Department of Biochemistry, Cancer Research Institute, Sapporo Medical University School of Medicine, S-1, W-17, Chuo-ku, Sapporo 060-8556, Japan. [4]Department of Cardiovascular Research, Research Institute of Environmental Medicine, Nagoya University, Furo-cho, Chikusa-ku, Nagoya 464-8601, Japan. [5]Laboratory Animal Center, Keio University School of Medicine, 35 Shinanomachi, Shinjuku-ku, Tokyo 160-8582, Japan. Correspondence should be addressed to K.F. (kfukuda@sc.itc.keio.ac.jp).

Received 9 November 2006; accepted 27 February 2007; published online 8 April 2007; doi:10.1038/nm1570

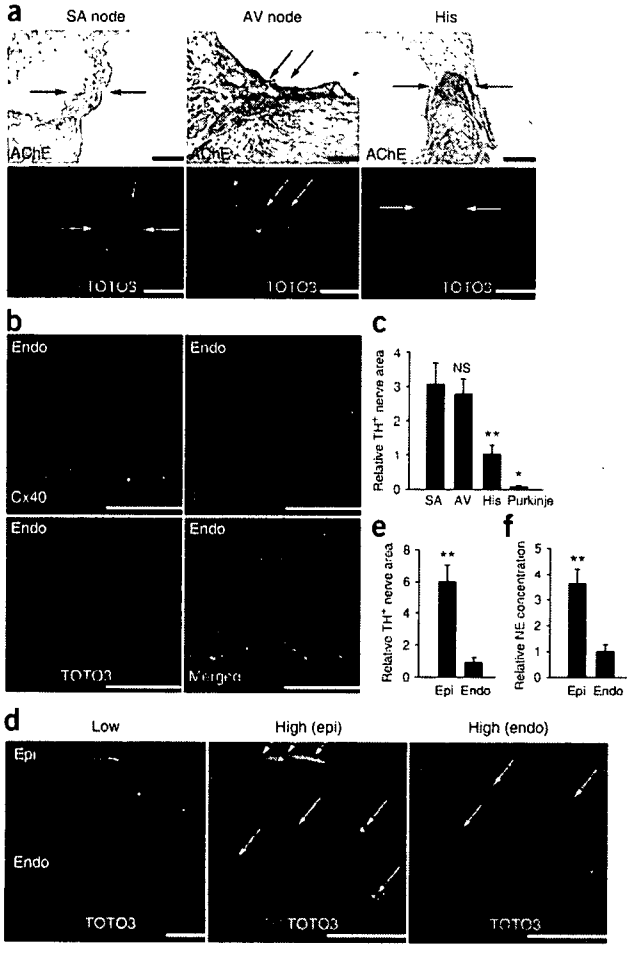

Figure 1 Regional heterogeneity of sympathetic innervation in the mouse heart. (**a**) The sinoatrial (SA) node, atrioventricular (AV) node and His bundle (arrows) stained with AChE (brown) were abundantly innervated by tyrosine hydroxylase–positive (TH^+) nerves. Top, acetyl cholinesterase (AChE) and hematoxylin staining. Bottom, immunofluorescent staining for α-actinin, tyrosine hydroxylase (TH) and TOTO3 (as a nuclear stain). (**b**) Immunofluorescent staining for α-actinin, TH, Cx40 and TOTO3 was performed. Few TH^+ nerves were detected in Purkinje fibers. (**c**) Quantitative analysis of TH^+ nerve areas ($n = 4$). (**d**) Immunofluorescent staining for α-actinin, TH and TOTO3. 'Low' and 'high' indicate low- and high-power fields, respectively. TH^+ nerves (arrows) were more abundant in the subepicardium (epi) than in the subendocardium (endo); quantitative data are shown in **e** ($n = 4$). (**f**) Cardiac norepinephrine (NE) concentration measured by high-performance liquid chromatography (HPLC) ($n = 6$). $^*P < 0.001$; $^{**}P < 0.01$; NS, not significant (in **c**, compared to SA). Scale bars, 100 μm.

fibers, which express connexin40 (Cx40)[20], were barely detectable and present in much smaller numbers than in the surrounding working myocardium (**Fig. 1b,c**). In the ventricular myocardium, TH^+ nerves were abundant and more so in the subepicardium than the subendocardium (**Fig. 1d,e**). The norepinephrine concentration was also significantly higher in the subepicardium (3.7-fold; **Fig. 1f**).

We next analyzed the time course of cardiac sympathetic innervation in developing mouse ventricles. Nerve endings appeared at embryonic day (E) 15 in the epicardial surface and were apparent in the myocardium at P7 and P42 (**Supplementary Fig. 1** online). Together, these results show that cardiac sympathetic nerve density exhibits regional differences, and that sympathetic nerve fibers in mice develop from the epicardial base of the heart into the myocardium, as observed in larger mammals[1,2,5].

Sema3a expression is inversely related to sympathetic innervation

To test whether Sema3a might be a signal for determining cardiac sympathetic innervation patterning, we analyzed heterozygous *Sema3a* knocked-in *lacZ* mice (*Sema3a*$^{lacZ/+}$) and determined *Sema3a* expression in the heart[16]. At E10, we observed *lacZ* expression in the forelimb buds and somites and weakly in the heart. *In situ* hybridization for *Sema3a* confirmed that *lacZ* expression in *Sema3a*$^{lacZ/+}$ mice correctly reflected endogenous gene expression (**Fig. 2a**). At E12, we detected strong *lacZ* expression in the heart, especially in the trabecular component of both ventricles (**Fig. 2b**). In E15 hearts, we observed *lacZ* expression at the subendocardium but not at the subepicardium in the atria and ventricles. At P1 and P42, *lacZ* expression was reduced in certain locations and highlighted the Purkinje fiber network along the ventricular free wall (**Fig. 2c**). To verify the presence of *lacZ*$^+$ cells in Purkinje fibers at P42, we immunostained sections with an antibody to Cx40 and found that ventricular subendocardial *lacZ*$^+$ cells also stained for Cx40 (**Fig. 2d**). In contrast, richly innervated and AChE-positive sinoatrial nodes (data not shown), atrioventricular nodes and His bundles did not express *lacZ* (**Fig. 2e**).

Quantitative RT-PCR of *Sema3a* in developing hearts also revealed that *Sema3a* mRNA was present from E12 and its levels then decreased in a linear fashion, in contrast to the sympathetic innervation (**Fig. 2f**). At P42, *Sema3a* mRNA expression was 2.3-fold higher in the subendocardium than in the subepicardium (**Fig. 2g**). These results indicated that *Sema3a* expression has an opposite time course and distribution from sympathetic innervation in developing hearts. Double staining with tyrosine hydroxylase and 5-bromo-4-chloro-3-indolyl-β-D-galactopyranoside (X-gal) revealed that most sympathetic nerves were restricted to the subepicardium at P1, when *Sema3a* was expressed extensively at the midcardial and subendocardial layers. At P42, sympathetic innervation extended vigorously into the ventricular myocardium, concomitant with *Sema3a* being downregulated and confined only to Purkinje fibers (**Fig. 2h**). Together, these results suggested that *Sema3a* is synthesized in Purkinje fibers and its expression is inversely related to the extent of sympathetic innervation.

Innervation patterning is disrupted in *Sema3a*$^{-/-}$ hearts

To investigate whether Sema3a is critical for cardiac sympathetic nerve development, we analyzed *Sema3a* homozygous null mice (*Sema3a*$^{-/-}$)[16]. Most *Sema3a*$^{-/-}$ mice die within the first postnatal week, and only 20% remain viable until weaning[16,17]. At P1, thick and fasciculated nerve fibers were restricted to the epicardial surface and few fibers were detected within the myocardium in the hearts of wild-type mice. In *Sema3a*$^{-/-}$ hearts, only a few fibers were observed at the epicardial surface, but many axons projected aberrantly into the myocardium at this early stage (**Fig. 3a,b**). To examine the overall pattern of cardiac sympathetic innervation, we performed whole-mount immunostaining for tyrosine hydroxylase at P1 on wild-type and *Sema3a*$^{-/-}$ hearts. Sympathetic nerve fibers appeared thinner and were fewer in number on the epicardial surface of *Sema3a*$^{-/-}$ hearts (**Fig. 3c**). At P14, when the sympathetic nerves extended into the myocardium, wild-type hearts showed a clear epicardial-to-endocardial gradient of sympathetic innervation. In contrast, sympathetic nerve density was reduced in the subepicardium but increased